JCB

Supplemental material

Hu et al., https://doi.org/10.1083/jcb.201812144

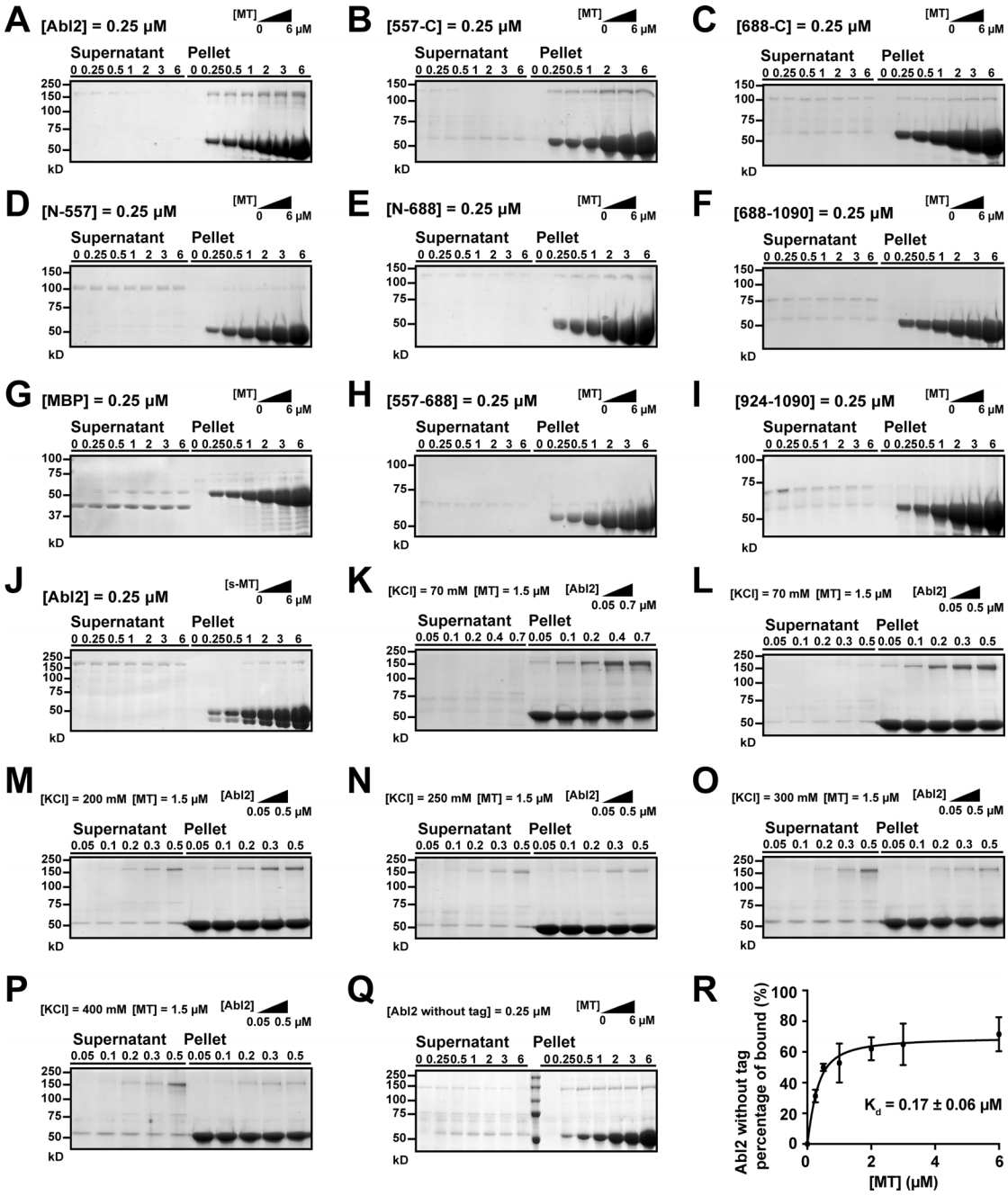

Figure S1. **SDS-PAGE gel images of MT/s-MT cosedimentation with Abl2 or Abl2 fragments. (A–I)** SDS-PAGE gel images of Abl2 or Abl2 fragments with MTs: A fixed concentration of 0.25 µM (A) Abl2, (B) 557-C, (C) 688-C, (D) N-557, (E) N-688, (F) 688–924, (G) MBP, (H) 557–688, or (I) 924–1090 was mixed with increasing concentrations of 0–6 µM MTs. The mixture was then pelleted by high-speed centrifugation, and the pellet and one third of the supernatant were separated by SDS-PAGE. The amount of Abl2 or Abl2 fragments in the supernatant and bound to MTs was quantified by densitometry for A–G). As MBP-tagged Abl2-557-688 or Abl2-924-1090 comigrates with MTs on SDS-PAGE, supernatant depletion of Abl2 fragments was used to infer MT binding. The amount of Abl2 fragments depleted from supernatant was quantified by densitometry for D, H, and I. Cropped images of Fig. S1, A–D, are shown in Fig. 1 A and Fig. 1 C. **(J)** SDS-PAGE gel image of Abl2 with s-MTs: A fixed concentration of 0.25 µM Abl2 was mixed with increasing concentrations of 0–6 µM s-MT. The mixture was then pelleted by high-speed centrifugation, and the pellet and one third of the supernatant were separated by SDS-PAGE. The amount of Abl2 in the supernatant and bound to MTs was quantified by densitometry. Cropped images of Fig. S1 J are shown in Fig. 1 E. **(K–P)** SDS-PAGE gel images of Abl2/MTs with increasing KCl concentrations: A fixed concentration of 1.5 µM MTs was mixed with increasing concentrations of (K) 0.05–0.7 µM Abl2 at 70 mM KCl or 0.05–0.5 µM Abl2 and increasing KCl concentrations of (L) 70 mM, (M) 200 mM, (N) 250 mM, (O) 300 mM, and (P) 400 mM. The mixture was then pelleted by high-speed centrifugation, and the pellet and one third of the supernatant were separated by SDS-PAGE. The amount of Abl2 bound to MTs was quantified by densitometry. Cropped images of Fig. S1, L–O are shown in Fig. 1 G. **(Q)** SDS-PAGE gel images of untagged Abl2 with MTs: A fixed concentration of 0.25 µM untagged Abl2 was mixed with increasing concentrations of 0 to 6 µM MTs. The mixture was then pelleted by high-speed centrifugation, and the pellet and one third of the supernatant were separated by SDS-PAGE. The amount of untagged Abl2 in the supernatant and bound to MTs was quantified by densitometry. **(R)** A plot of the percentage of untagged Abl2 bound to MTs is shown. Untagged Abl2 binds to MTs with a K_d = 0.30 ± 0.07 µM (mean ± SD). Error bars are presented as mean ± SD, n = 3. The R^2 value for curve fitting is 0.90.

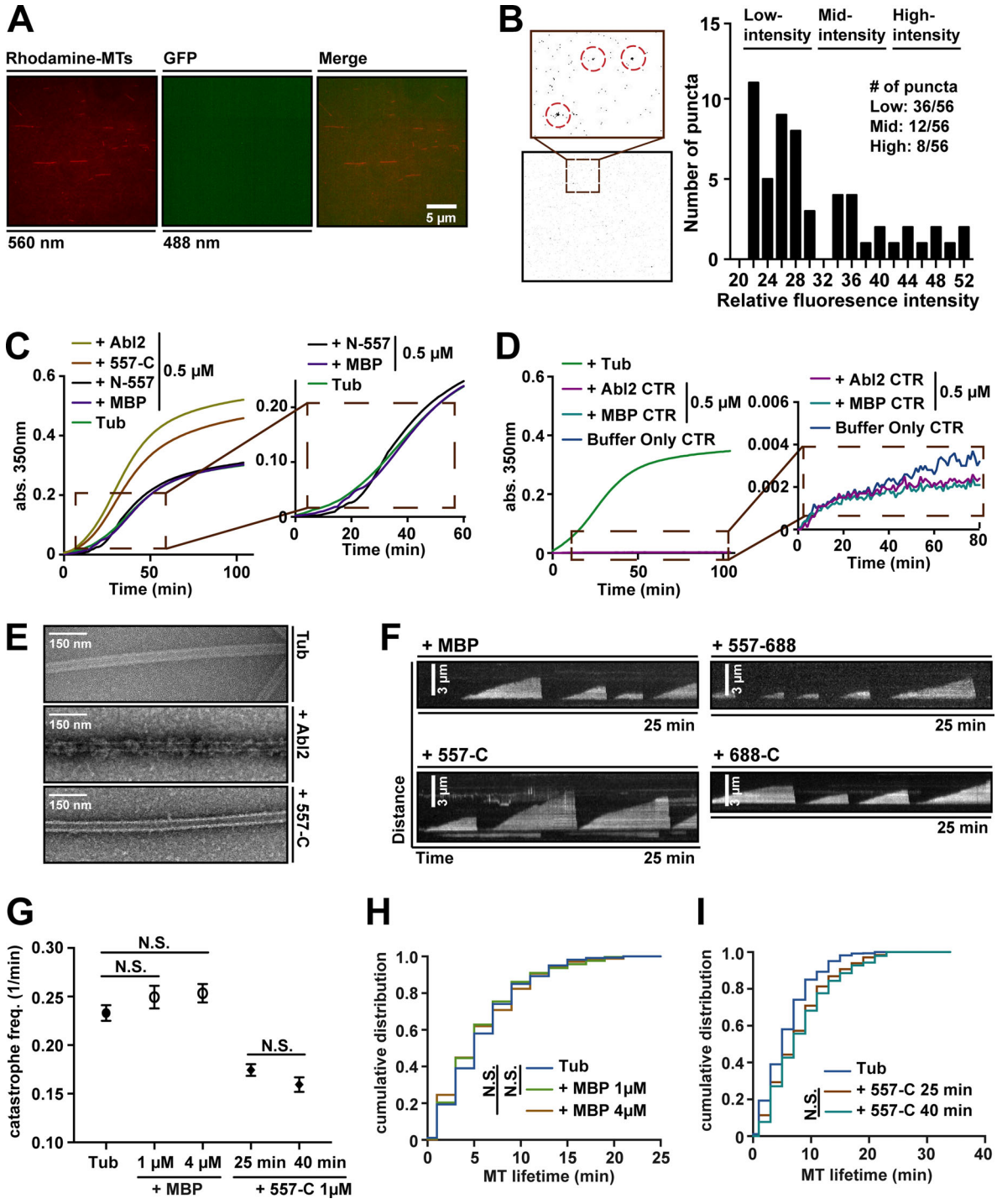

Figure S2. **In vitro TIRF imaging and turbidity measurements of tubulin assembly. (A)** Rhodamine-labeled GMPCPP-stabilized MTs (red) bound to the coverslip with anti-rhodamine antibodies in the flow chamber were observed using TIRF microscopy in red (560 nm) and green (488 nm) modes. **(B)** Fluorescence intensities of individual Abl2-557-C-GFP puncta were measured with 20 nM Abl2-557-C-GFP in the flow chamber. Puncta were categorized into Low-, Mid-, and High-intensity groups based on fluorescence intensity. **(C)** The amount of total assembled tubulin was monitored by measuring turbidity at 350 nm (A350). 18 µM tubulin was incubated with 1 mM GTP in BRB80 buffer alone (Tub) or with 0.5 µM Abl2, Abl2-557-C, Abl2-N-557, or MBP. **(D)** One representative time series of A350 measurements for buffer alone (Buffer Only Control [CTR]), buffer with only Abl2 or MBP (+ Abl2 CTR or + MBP CTR), or buffer with only 18 µM tubulin (+ Tub) are shown. **(E)** Negative stain electron microscopy images of samples taken at the end of the turbidity assay: tubulin alone (Tub), tubulin with 0.5 µM Abl2 (+ Abl2), or tubulin with 0.5 µM Abl2-557-C (+ 557-C). **(F)** Kymographs of MT dynamics incubated 7 µM Alexa 488–tubulin with 1 µM MBP, Abl2-557-C, Abl2-557-688, or Abl2-688-C. **(G)** To determine possible effects of MBP on MT dynamics, 7 µM Alexa 488–tubulin was incubated with 1 or 4 µM MBP in imaging buffer, and MT catastrophe frequencies were measured for 25 min at 0.2 FPS. To measure possible effects of imaging time, 7 µM Alexa 488–tubulin was incubated with 1 µM Abl2-557-C in imaging buffer, and MT catastrophe frequencies were measured for 25 min at 0.2 FPS or 40 min at 0.1 FPS. Quantifications were based on kymographs of individual MT behaviors. **(H and I)** The cumulative frequencies of individual MT growth time were plotted for (H) MBP control, or (I) imaging time control. Error bars are presented as mean ± SEM, $n \geq 100$. N.S., not significant.

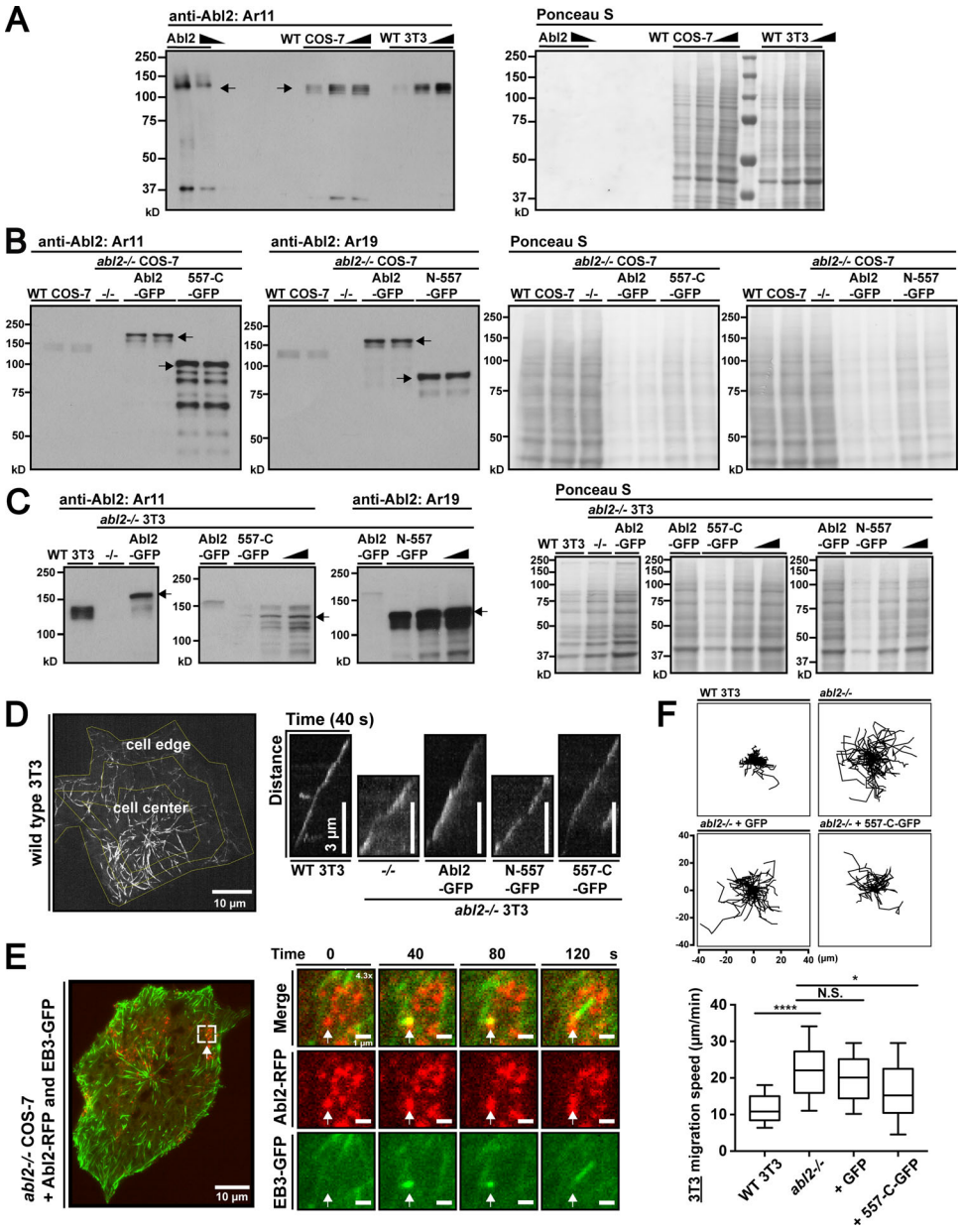

Figure S3. **Western blots of Abl2 or Abl2 fragments in COS-7 and mouse 3T3 fibroblast cells, kymograph analyses of MT growth in 3T3 cells, and COS-7 cells reexpressing EB3-GFP and Abl2-RFP, 3T3 cell migration analyses. (A)** Ar11 immunoblot of recombinant Abl2, WT COS-7 cell lysate, and WT mouse 3T3 fibroblast cell lysate. Ar11 recognizes the C-terminal half of Abl2. The expected bands of Abl2 (134 kD) are indicated. Ponceau S staining reveals the total amount of the protein loaded in each lane (purified recombinant Abl2: 0.08 and 0.053 µg, WT COS-7: 10, 20, 30 µg, WT 3T3: 10, 20, 30 µg). **(B)** Ar11 immunoblot of WT and *abl2*$^{-/-}$ COS-7 cells, and *abl2*$^{-/-}$ COS-7 cells reexpressing Abl2-GFP or Abl2-557-C-GFP. Ar19 immunoblot of WT and *abl2*$^{-/-}$ COS-7 cells, and *abl2*$^{-/-}$ COS-7 cells reexpressing Abl2-GFP and Abl2-N-557-GFP. Ar19 recognizes the Abl2 N-terminal half. The expected bands of Abl2, Abl2-GFP (161 kD), Abl2-557-C-GFP (96 kD), and Abl2-N-557-GFP (92 kD) are indicated. Ponceau S staining reveals the total amount of the protein loaded in each lane of the Ar11 blot (WT COS-7: 30, 30 µg, *abl2*$^{-/-}$ COS-7: 30 µg, *abl2*$^{-/-}$ COS-7 + Abl2-GFP: 5, 5 µg, *abl2*$^{-/-}$ COS-7 + Abl2-557-C-GFP: 5, 5 µg) and the Ar19 blot (WT COS-7: 30, 30 µg, *abl2*$^{-/-}$ COS-7: 30 µg, *abl2*$^{-/-}$ COS-7 + Abl2-GFP: 5, 5 µg, *abl2*$^{-/-}$ COS-7 + Abl2-N-557-GFP: 5, 5 µg). **(C)** Left: Ar11 immunoblot of WT mouse 3T3 fibroblast cells, *abl2*$^{-/-}$ 3T3 cells, and *abl2*$^{-/-}$ 3T3 cells reexpressing Abl2-GFP. Center: Ar11 immunoblot of *abl2*$^{-/-}$ 3T3 cells reexpressing Abl2-GFP or Abl2-557-C-GFP. Right: Ar19 immunoblot of *abl2*$^{-/-}$ 3T3 cells reexpressing Abl2-GFP or Abl2-N-557-GFP. The expected bands of Abl2, Abl2-GFP, Abl2-557-C-GFP, and Abl2-N-557-GFP are indicated. Ponceau S staining reveals the total amount of the protein loaded in each lane of the left Ar11 blot (WT 3T3: 20 µg, *abl2*$^{-/-}$ 3T3: 20 µg, *abl2*$^{-/-}$ 3T3 + Abl2-GFP: 50 µg), the center Ar11 blot (*abl2*$^{-/-}$ 3T3 + Abl2-GFP: 30 µg, *abl2*$^{-/-}$ 3T3 + Abl2-557-C-GFP: 10, 20, 30 µg), and the right Ar19 blot (*abl2*$^{-/-}$ 3T3 + Abl2-GFP: 30 µg, Abl2-N-557-GFP: 10, 20, 30 µg). **(D)** Maximum intensity projection of the MT plus-tip tracker, mCherry-MACF43, showed single MT tracks in a WT 3T3 cell. Kymographs of MT plus-tip growth at the cell edge in WT and *abl2*$^{-/-}$ 3T3 cells, and in *abl2*$^{-/-}$ 3T3 cells reexpressing Abl2-GFP, Abl2-N-557-GFP, or Abl2-557-C-GFP are shown. For reference, the kymographs of WT and *abl2*$^{-/-}$ cells, and *abl2*$^{-/-}$ 3T3 cells reexpressing Abl2-GFP are reproduced here from Fig. 4 E. **(E)** Maximum intensity projection of an *abl2*$^{-/-}$ COS-7 cell expressing EB3-GFP and Abl2-RFP. Time-lapse shots showed MT plus-tip tracker, EB3-GFP, and Abl2-RFP puncta. **(F)** Cell migration tracks showed the displacements of WT and *abl2*$^{-/-}$ 3T3 fibroblasts, and *abl2*$^{-/-}$ 3T3 cells reexpressing Abl2-557-C-GFP or GFP over 6 h. The plot showed the speed of migration. Error bars are presented as mean ± SD $n \geq 30$. *, $P < 0.05$; ****, $P < 0.0001$. N.S., not significant.